Journal of Applied Polymer Science

Morphology development and size control of PA6 nanofibers from PA6/CAB polymer blends

Peipei Zhang, Dandan Xu, Ru Xiao
State Key Laboratory for Modification of Chemical Fibers and Polymer Materials, College of Materials Science and Engineering, Donghua University, Shanghai 201620,
People's Republic of China
P. Z. and D. X. contributed equally to this work.
Correspondence to: R. Xiao (E-mail: xiaoru@dhu.edu.cn)

ABSTRACT: Polyamide 6 (PA6) nanofibers were prepared by the melt blending extrusion process of PA6/cellulose acetate butyrate (CAB) immiscible polymer blends. The average diameter of obtained PA6 nanofibers was 95–190 nm which could be controlled by varying the process conditions, such as blend ratio was 10/90-40/60, shear rate was 10 and 80 $s^{-1}$and two different blending equipments, and the effect of adding graphene for the diameters was also discussed. In addition, and the formation mechanism of nanofibers was studied by viscoelastic analysis and collecting samples at four different sites along the extruder. The morphology of PA6 dispersed phase in CAB matrix included three stages: PA6 pellets changed into sheets or ribbons, the formation of microfibers and size reduction, the size of microfibers continued refinement to nanofibers. The morphology development of dispersed phase may be postponed by blend ratio. © 2015 Wiley Periodicals, Inc. J. Appl. Polym. Sci. **2015**, *132*, 42184.

KEYWORDS: blends; morphology; polyamides

Received 24 November 2014; accepted 13 March 2015
DOI: 10.1002/app.42184

INTRODUCTION

Nanofibers have a wide range of applications, such as efficient filtration devices, surgical dressing and tissue scaffolds etc., because of its large surface area and good biocompatibility,[1,2] the preparation methods and the research of nanofibers has a growing improvement. So far, many developed production methods can be used to prepare micro-nano fibers, including electrospinning,[3] drawing, meltblowing, flash spinning and sea-island spinning, but some of these methods have difficult to produce fibers with averaged diameters less than 500 nm.[4] The melt blending extrusion is also a method for preparing nanofibers,[5–9] which can be described as a kind of phase separation behavior of immiscible system with simple equipment, high yield and environmental protection. Many researchers have studied the effect on the morphology development of dispersed phase in polymer blends, such as the content of blends,[10] the compatibility of blends,[11] the viscosity ratio, the shear rates,[12] and the blend ratio.[13] Sundararaj had studied the morphology development of PS/PA and PS/PP blends and found the size of dispersed phase reduced mainly in melting stage.[14] Scott etc. had studied the morphology development of polymer blends during the initial stages of blending in different blending equipment, and proposed mechanism for initial morphology development in polymer blends.[15–17] Elemans had researched the structure development of PA6/PP and proposed polymer initial structure development mechanism by mechanical blending.[18] Polyamide 6 (PA6) is a kind of material with the performance of high strength, light, wear-resisting, high elastic recovery rate, etc. However, due to the high viscosity, slightly solubility and easy degradation in high temperature, the preparation of PA6 superfine fiber is limited.[19] Besides, researches on PA6 nanocomposites such as graphene/PA6 matrix, which has recently attracted considerable interest.[20–22]

This article discussed the preparation of PA6 nanofibers by the melt blending extrusion process. It involved choosing two kinds of immiscible thermoplastic polymers, mixing and extruding from a twin-screw extruder. After removing the cellulose acetate butyrate (CAB) matrix, nanofibers could be obtained. To control the size of PA6 nanofibers, several parameters were studied, such as blend ratio, shear rate, and blending equipment. Besides, the viscoelastic of blends and the morphology

Additional Supporting Information may be found in the online version of this article.

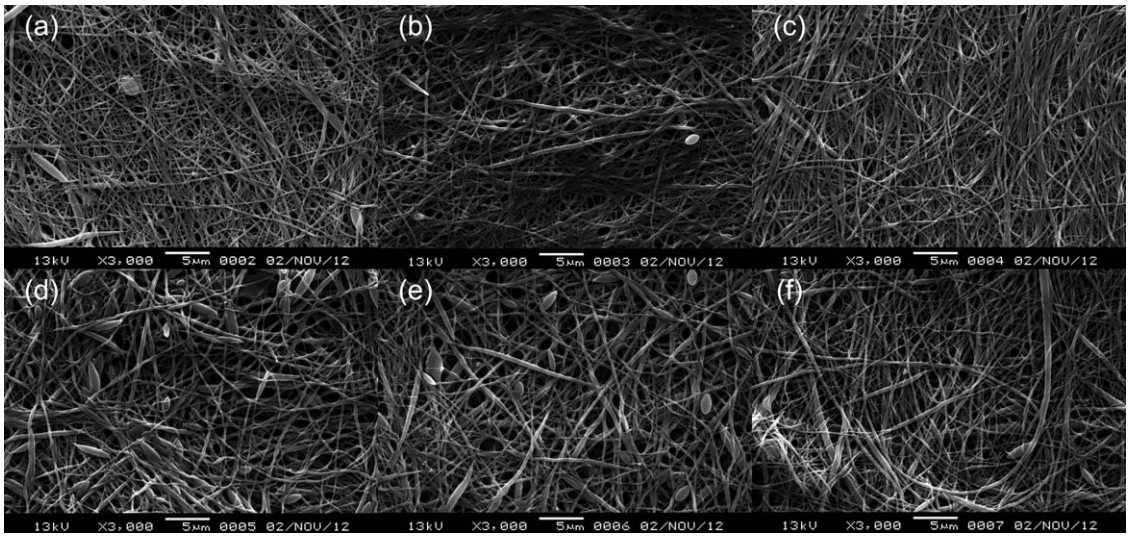

Figure 1. SEM images of the graphene/PA6 composite nanofibers prepared by micro-twin screw blender with graphene percentage of 0.1, 0.3, 0.5, 1, 3, 5wt % (a–f).

development of dispersed phase in extruding process had also been discussed. To study the application of PA6 nanofibers, the work also studied the effect of adding graphene for PA6 fiber diameters

EXPERIMENTAL

Materials

Polyamide 6 (PA6, M32800), relative viscosity: 2.8 (1 g/100 mL 98% H_2SO_4 at 20°C), provided by Guangdong Xinhui Meida nylon Company. CAB powder (CAB-171-15, butyryl content 17 wt %, acetyl content 19.5% and hydroxyl content 1.5 wt %), purchased from Eastman chemical (U.S.), used as a matrix phase. The melting point of CAB is 230–240°C. Graphene was prepared using graphite as raw material by ourselves. PA6 and CAB were dried in a vacuum oven at 120°C for 48 h, and graphene was dried in a vacuum oven at 65°C for 24 h before blending.

Preparation

PA6 and CAB were blended by using a co-rotating twin-screw extruder ($D = 16$ mm, $L/D = 40$, EUROLAB16, Thermo-Harke Co.) to prepare PA6/CAB composite. The processing temperature was mainly based on polymer thermal performance. The twin-screw extruder has three different sampling points, named SP-1#, SP-2#, and SP-3# To study the melting and the morphology evaluation of the blends along the extruder, the samples were collected from these three points, which represent the morphology at different times respectively. The samples, taken from the extruder, were immediately cooled by putting in the ice water to retain the morphology that developed in the extruder.

The factors on the morphology and diameter size of the PA6 dispersed phase was discussed, like viscoelasticity and blend ratio of blends, shear rate of screw and mixing facility. The blend ratio between PA6 and CAB was set at 10/90, 15/85, 20/80, 30/70, and 40/60, while the shear rate was 50 s^{-1} and draw ratio was 9. In the study of the shear rate, the screw shear rate varied at 10, 30, 50, 80, 100, and 120 s^{-1}, while the blend ratios was 20/80 and draw ratio was 9. PA6 mixed with CAB by Harke co-rotating twin-screw extruder and miniature twin-screw blend instrument (HLYB/8-C5, $D = 8$ mm, $L/D = 12$ mm) at the same shear rate of 50 s^{-1} with blend ratio of 10/90, 20/80, 30/70, and 40/60 was studied. Graphene/PA6 composites were prepared by blending Graphene and PA6, then Graphene/PA6 composites and CAB were mixed with the blend ratio of 20/80 by miniature twin-screw blend instrument. All the samples were extracted by immersing the samples in exchanged acetone at room temperature till removed the matrix component CAB completely. It was confirmed by the FT-IR results of PA6, CAB, and PA6 nanofibers after removing the matrix (shown in Supporting Information Figure S1).

Measurement and Characterization

The apparent viscosity and elastic modulus of the polymer were both determined by using a dynamic rheometer (ARES-RFS) with a 25-mm parallel plate under the static and dynamic mode respectively. The rheological measurements of PA6/CAB system were performed at 250°C.

The morphology of samples in the extruder and the final obtained nanofibers were observed by a scanning electron microscope (SEM). To observe the fracture surfaces of the composite fibers, the composites were fractured in liquid nitrogen and were observed by SEM.

The distributions and averages of the fibers' diameters were obtained by measuring 100 nanofibers. The number of averaged diameters was calculated as eq. (1).

$$D_N = \frac{\sum N_i D_i}{\sum N_i} \quad (1)$$

in which, D_N is the number averaged diameters and N_i is the number of nanofiber with a diameter of D_i.

Table I. Diameter Statistics of Graphene/PA6 Nanofibers with Different Graphene Percentage

Samples	Smallest diameter (nm)	Largest diameter (nm)	Average diameter (nm)
0 wt % GN/PA6	63	241	123
0.1 wt % GN/PA6	57	349	141
0.3 wt % GN/PA6	57	279	135
0.5 wt % GN/PA6	63	358	166
1 wt % GN/PA6	100	471	209
3 wt % GN/PA6	100	456	228
5 wt % GN/PA6	94	612	249

RESULTS AND DISCUSSION

Effect of Graphene

PA6/CAB and graphene/PA6/CAB composites were both collected directly from the twin-screw extruder by melt blending and extrusion. PA6 nanofibers and PA6/graphene composite nanofibers were obtained by removing the matrix component CAB completely. Compatibility directly impacted the morphology and structure of polymer blends, the formation of nanofibers was determined by the shape and size of dispersed phase.

Figure 1 shows the SEM images of the graphene/PA6 composite nanofibers prepared by micro-twin-screw blender with different percentage of graphene and also suggests that the PA6/graphene composite nanofibers could be prepared by melt blending effectively. What's more, the average diameters of graphene/PA6 nanofibers were raised with increased percentage of graphene. Diameter distribution of graphene/PA6 nanofibers with graphene percentage of 0, 0.1, 0.3, 0.5, 1, 3, 5 wt % were shown in Supporting Information Figure S2(a–g) and Table I, and the effect of graphene percentage on nanofibers average diameters was shown in Supporting Information Figure S2(h). This is due to the addition of graphene increased the interfacial tension between PA6 and CAB, so decreased the compatibility. Meanwhile, the addition of graphene increased the crystalline temperature and improved the thermal stability of graphene/PA6 composite nanofibers (shown in Supporting Information Figures S3, S4, S5 and Supporting Information Table SI).

Effect of Blend Ratio

Figure 2 shows the fracture surface of PA6/CAB composites with different blend ratio. Figure 3 shows the PA6 nanofibers prepared by Harke co-rotating twin-screw extruder with different blend ratio. In the Figure 2(a–d), the two phases have obvious interface and immiscible completely. The dispersed phases PA6 in the continuous CAB matrix formed an apparent sea-island structure. With the increase of the percentage of PA6, the probability of particle collision increased correspondingly. When the blend ratio of PA6/CAB was 50/50, the interface between phases was so ambiguous that we couldn't distinguish the dispersed phase from matrix phase. After removing the CAB matrix, the fibrous dispersed phase was obtained. As shown in Figure 3(a–d), with increasing PA6 component loading level, the morphology of dispersed spherical droplets in the continuous phase changed into fibrous and finally to the co-continuous structure. Well-defined PA6 nanofibers could be obtained at the blend ratio of 10/90-40/60.

Figure 4 shows the variation of PA6 nanofibers' average diameter due to the different blend ratio. With the percentage of PA6 increased from 10 to 40 wt %, the average diameter of PA6 nanofibers showed an increasing tendency as expected, which were 95, 97, 105, 112, 178 nm, respectively, so did the distribution of fiber average diameters. The mainly reason was the collisional coalescence of PA6 droplets during the melt-extruding process, which was known as a random process and enhanced collision with the increasing of the blend ratio, hence raising the diameters of PA6 nanofibers and broadening the diameter distribution.

Effect of Shear Rate

Shear rate facilitates the deformation of the dispersed phase and could affect the viscoelasticity of the polymer blends during the

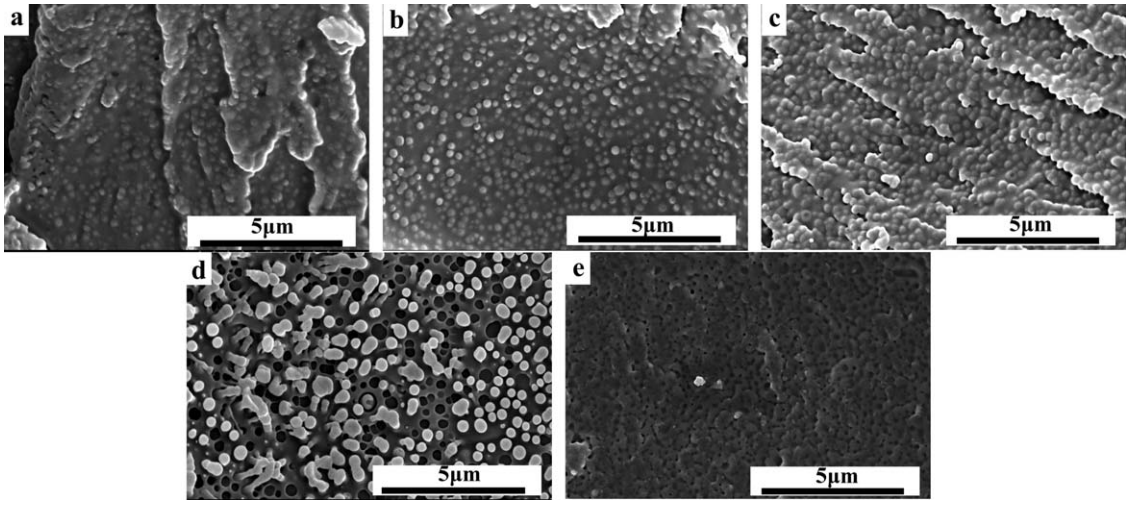

Figure 2. SEM images of fracture surface of PA6/CAB blends prepared by Harke co-rotating twin-screw extruder with different blends ratio. (a) 10/90, (b) 20/80, (c) 30/70, (d) 40/60, (e) 50/50.

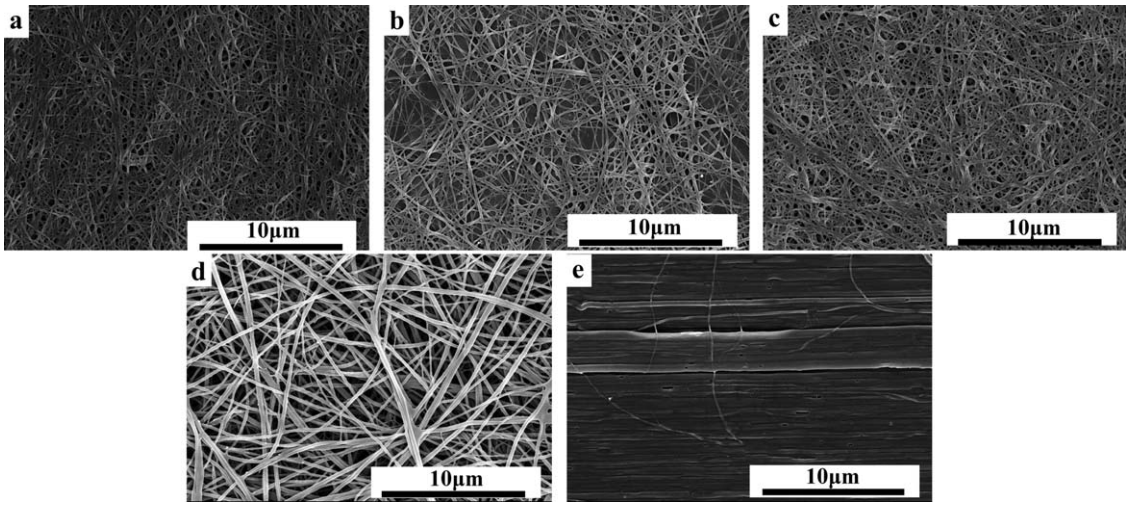

Figure 3. SEM images of PA6 nanofibers prepared by Harke co-rotating twin-screw extruder with different blend ratio, (a) 10/90, (b) 20/80, (c) 30/70, (d) 40/60, (e) 50/50.

melt blending process. It is one of the important parameters for the formation of nanofibers in melt extruding. On the one hand, higher shear rate promoted deformation and breaking of dispersed phase pellets and reduced the coalescence of dispersed micelles,[23] thereby leading to the dispersed phase size decreased. On the other hand, increasing the shear rate could improve the viscosity and elastic ratio between disperse phase and matrix, which went against deformation and breaking of the dispersed phase particles.[24] Therefore, the effect of shear rate on the shape and the size of dispersed phase was multiple.

Figures 5 and 6 shows the morphology and corresponding diameter distribution of nanofibers from PA6/CAB blends at different shear rates. The average diameter of PA6 nanofibers were 188, 131, 105, 100, 101 nm with the shear rate of 10, 30, 50, 80, 120 s^{-1}, respectively. When the shear rate gradually increased from 10 s^{-1} to 80 s^{-1}, the diameter of nanofibers became well-distributed and smaller apparently. While continued to increase the shear rate, the diameter appeared upwards trend. This was the multiple influence of shear rate on the dispersed phase. Researches suggested that the shear rate had a critical maximum and minimum value in the dispersed droplet microfibrillar blend process.[25–28] When shear rate below the critical minimum value, droplet did not deform; while higher than the critical maximum value, the micro fiber could not remain stable, but easy to break into smaller droplets.[23]

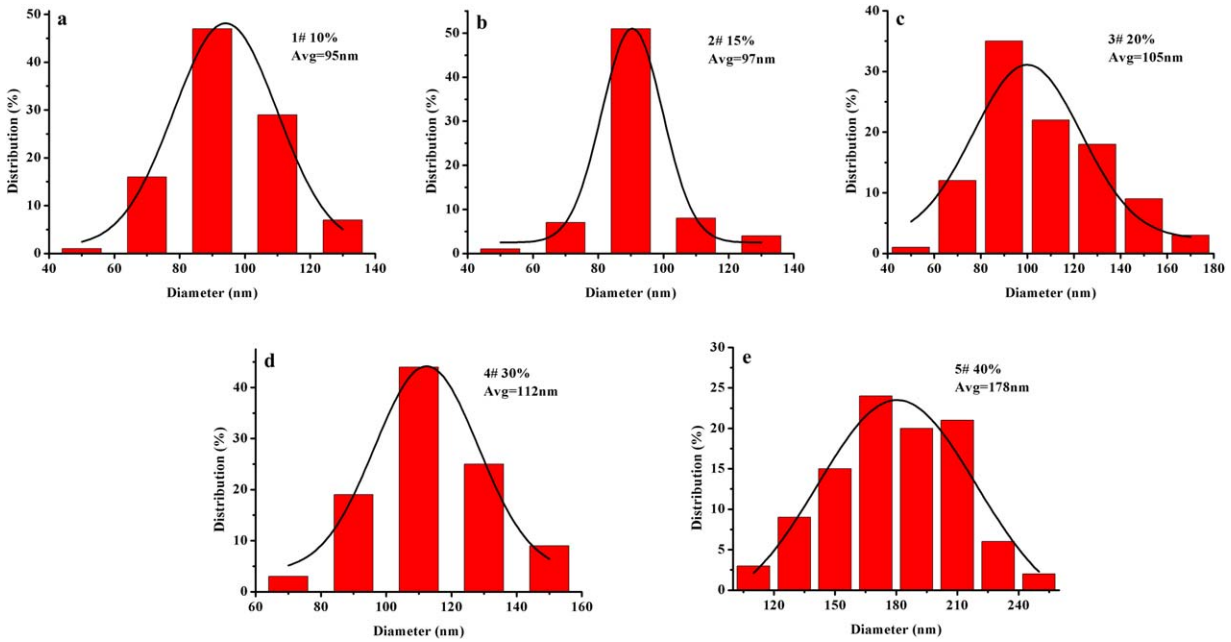

Figure 4. Diameter distribution of PA6 nanofibers prepared by Harke co-rotating twin-screw extruder with different blend ratio. (a) 10/90, (b) 15/85, (c) 20/80, (d) 30/70, (e) 40/60. [Color figure can be viewed in the online issue, which is available at wileyonlinelibrary.com.]

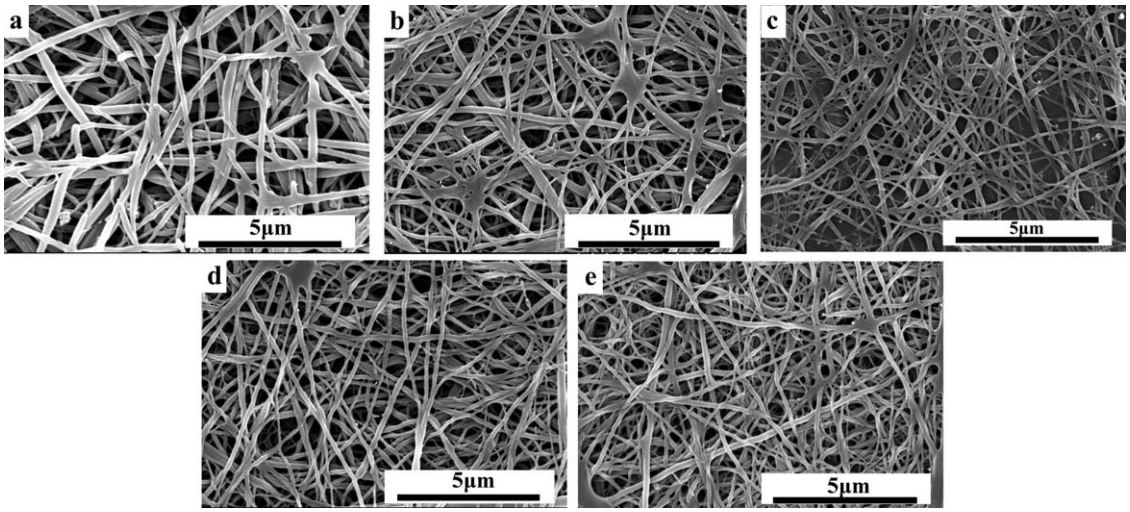

Figure 5. SEM images of PA6 nanofibers prepared by Harke co-rotating twin-screw extruder with different shear rates. (a) $10s^{-1}$, (b) $30s^{-1}$, (c) $50s^{-1}$, (d) $80s^{-1}$, (e) $120s^{-1}$.

Effect of Blending Equipment

The morphology and size of immiscible polymer blends could be influenced greatly by the blending equipment, so did the nanofibers. Because different blending equipment have different flow field, blending time and shear capacity. It is known that blending equipment contain several parameters impacted on the final melt-extruding results. In this article, the diameter (D) and length to diameter ratio (L/D) of screw were mainly parameters to be considered.

Figures 7 and 8 illustrated the melt-extruding results got by micro-twin-screw blender which were similar to the harke co-rotating twin-screw extruder, that PA6 nanofibers could be formed at the blend ratio of 10/90, 20/80, 30/70, and 40/60 except 50/50. With the increasing of blend ratio, the average diameter of nanofibers increased gradually in according with the result from Harke co-rotating twin-screw extruder.

However, nanofibers obtained by micro-twin-screw blender significantly had bigger diameter and broader diameter distribution than those obtained by Harke. Figure 8(e) showed PA6 nanofibers diameter curves had the same variation trend. However, in the case of same blend ratio change, the diameter variation of nanofibers obtained by micro screw blending was smaller. It could be concluded that micro screw blending was less sensitive to blend ratio compared with Harke blending. The different results out of the two blending equipment was mainly due to the different inner structure of the equipment.

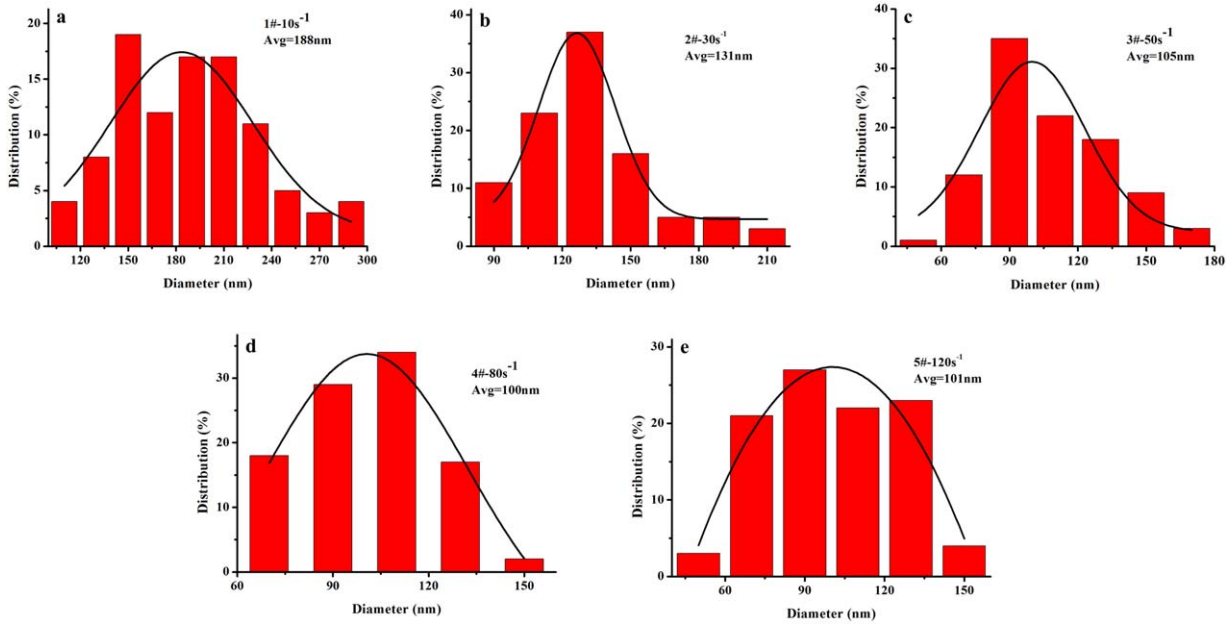

Figure 6. Diameter distribution of PA6 nanofibers prepared by Harke co-rotating twin-screw extruder with different shear rates. (a) $10s^{-1}$, (b)30 s^{-1}, (c) $50s^{-1}$, (d) $80s^{-1}$, (e) $120s^{-1}$. [Color figure can be viewed in the online issue, which is available at wileyonlinelibrary.com.]

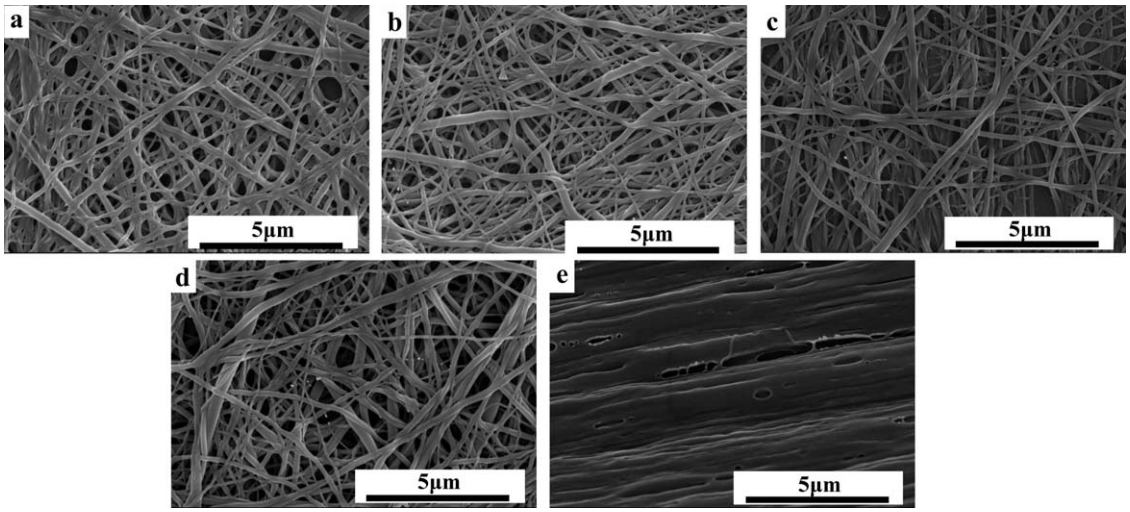

Figure 7. SEM images of PA6 nanofibers prepared by micro-twin-screw blender with different blend ratio, (a) 10/90, (b) 20/80, (c) 30/70, (d) 40/60, (e) 50/50.

Formation Mechanism

Melt-extruding process involved shear flow and elongational flow field.[1,2] The final obtained PA6 nanofibers that were the result out of the combined action with continuous deformation broken and coalescence of PA6 dispersed droplets into CAB matrix. Polymer was viscoelastic, hence the morphology of dispersed phase was either associated with viscosity or elasticity. Viscosity ratio η_d/η_m (η_d is the viscosity of the dispersed phase, η_m is the viscosity of the matrix phase) played an important part on the deformation process of dispersed phase. The effect of η_d/η_m on the fibril formation has been discussed. Plate *et al.* studied 13 different pairs of polymers and concluded that dispersed phase could fibrillated in the matrix when the η_d/η_m value between 0.1 and 10.[27]

Complex viscosity and storage modulus were tested to characterize the rheological property of PA6/CAB blends. Figure 9(a) showed complex viscosity (η^*) of PA6 and CAB and corresponding viscosity ratio (η_d/η_m) as the function of frequency. Figure 9(b) showed the curves of storage modulus (G′) of PA6, CAB, and PA6/CAB blends as the function of frequency. Complex viscosity was almost the same at low frequency. With the increasing of shear rate, η^* decreased continuously, indicated that PA6 and CAB were both non-Newtonian liquid with shear thinning. The viscosity ratio of PA6 and CAB was between 5.9

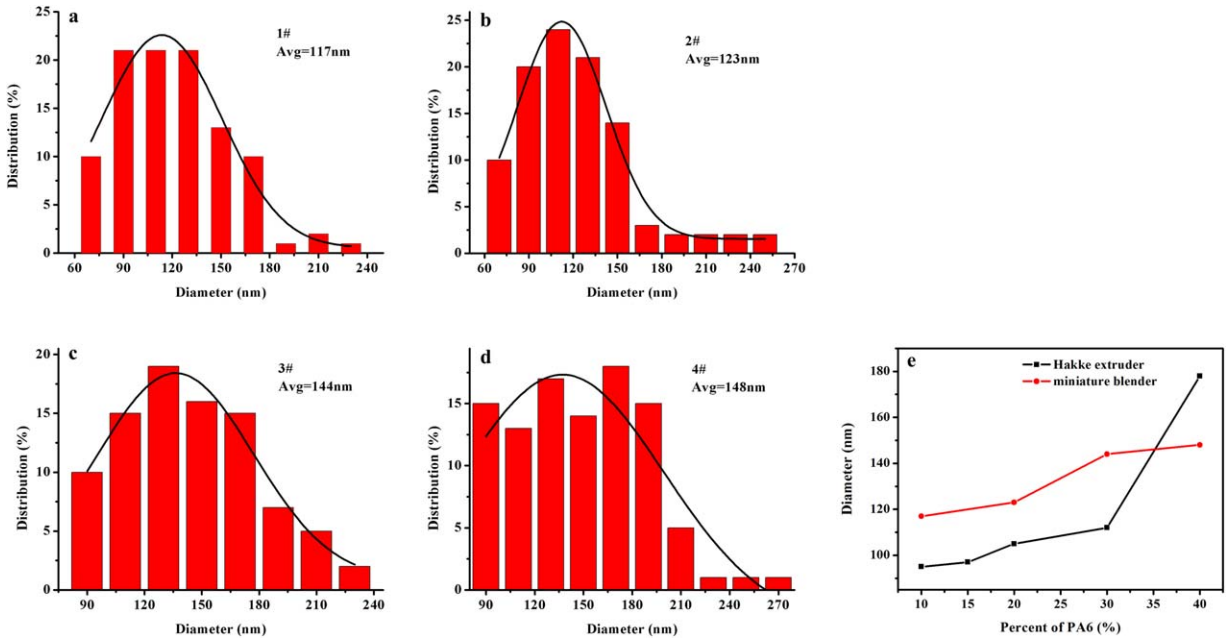

Figure 8. Diameter distribution of PA6 nanofibers prepared by micro-twin-screw blender with different blend ratio (a) 10/90, (b) 20/80, (c) 30/70, (d) 40/60, (e) curve of average diameters of PA6 nanofibers obtained by two kinds of blending equipment. [Color figure can be viewed in the online issue, which is available at wileyonlinelibrary.com.]

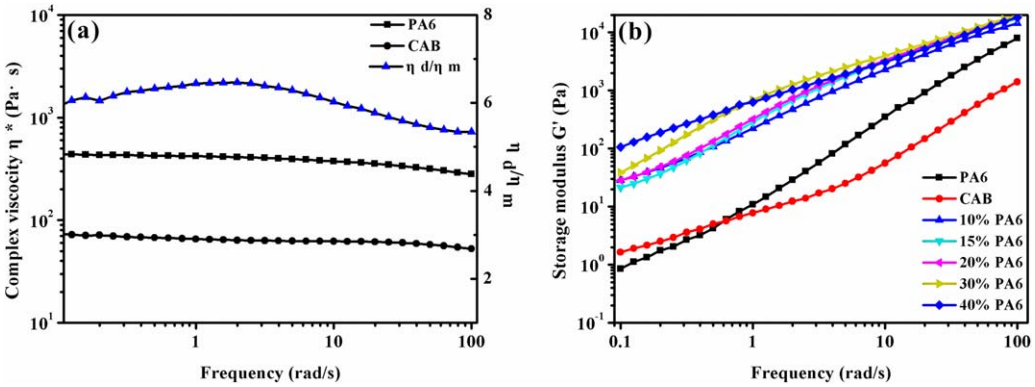

Figure 9. Frequency dependence of (a) complex viscosity, viscosity ratio and (b) elastic modulus for PA6/CAB blends at 250°C. [Color figure can be viewed in the online issue, which is available at wileyonlinelibrary.com.]

and 6.5, implying that the morphology of dispersed phase were able to be fibrous. Besides, the elastic modulus of CAB was higher than PA6 in the low frequency region, so the matrix had a higher elasticity than dispersed phase. The elasticity of matrix could promote fiber formation and enhance the stability of dispersed fibers. In the high frequency region, the elastic modulus of PA6/CAB blends increased with the increasing of the content of PA6. Higher G' was unfavorable for the deformation of the dispersed phase, made the diameters of fibril bigger, so that the average diameters of nanofibers were bigger with the increasing of the content of PA6. The conclusion was coincided with the result of the effect of blend ratio.

The PA6/CAB blends in extruder successively experienced melt, blend and extruding under the combined action of shear and elongational flow. So the morphology of dispersed phase in different stage of twin-screw extruder was different. Figure 10 showed the morphology development of PA6 dispersed phase with different blend ratio after removing matrix. As is shown in Figure 10, the extruder has three sampling site SP-1#, SP-2#, and SP-3#, corresponded to the initial stage, metaphase, and

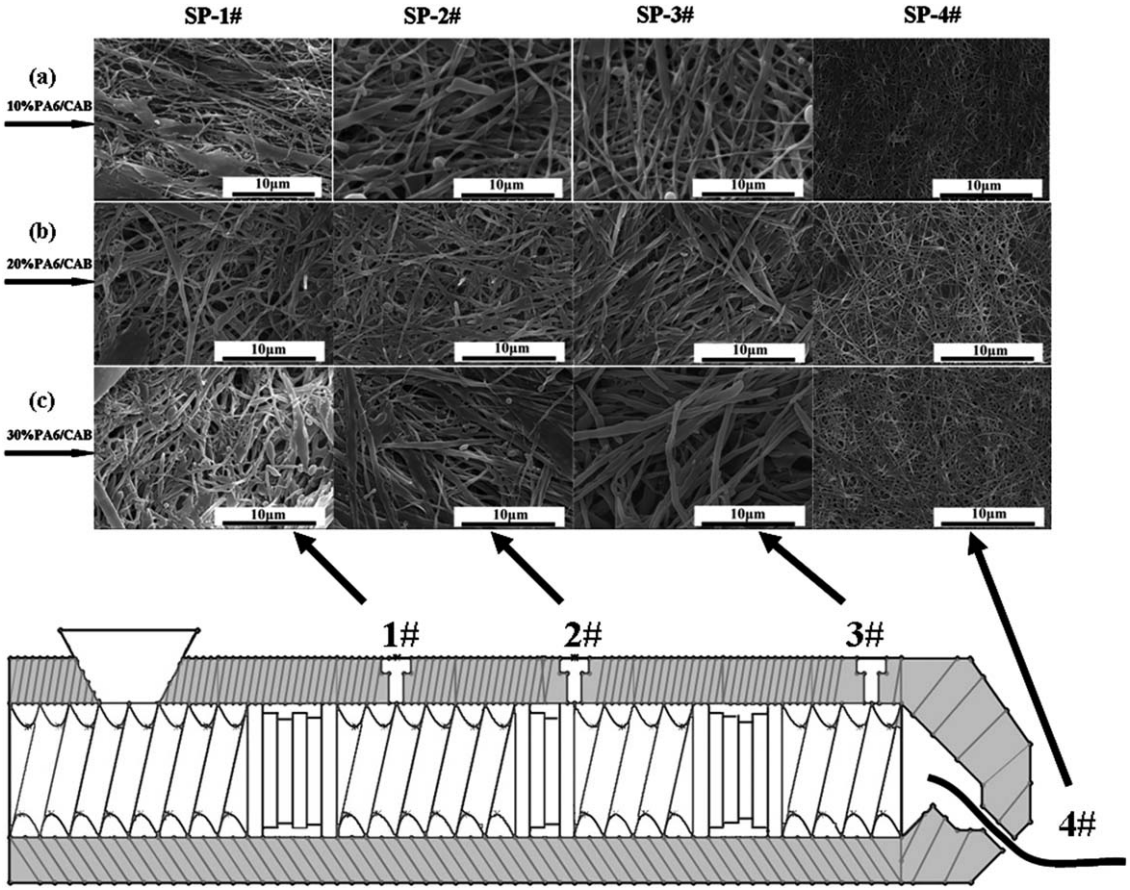

Figure 10. SEM images of morphology development of PA6 dispersed phase with different blend ratio.

later morphological development of the blends respectively. SP-4# was the morphology of dispersed phase after extruding and elongation. In SP-1# sampling site, the dispersed PA6 of blend system a (10%PA6/CAB) and b (20%PA6/CAB) mainly existed in the morphology of sheets and ribbons, while the morphology of blend system c were pellets, ellipsoids and ribbons. The quick morphological changes in the initial stage of blend were related to particle crushing mechanism. The different morphology between blends system were due to blend ratio. According to the rheological property, higher components of PA6 increased η_d/η_m but reduced the shear action between matrix and dispersed phase, thus hindered the deformation of dispersed pellets. Besides, prolonged melting time was another reason. In the metaphase, blends were melted completely and the mixing efficiency was better. The ribbons mostly changed into fibrous under the continuous shearing action except that sample (c) still had some small sheets. The later stage was the refinement of micro fibers but the morphology changed little. The micro fibers deformed accompany with shrinkage. The final nanofibers were the overall results of deformation, shrinkage and elongation. The morphology could be concluded as follows: the initial morphology development stage was the dispersed phase PA6 changed from pellets to sheets or ribbons, the metaphase stage was the formation of PA6 micro fibers and the later stage was the refinement of micro fibers. Besides, higher blend ratio may put off the morphology development procedure and make the diameters of fibril bigger.

CONCLUSIONS

PA6 nanofibers were prepared from PA6/CAB immiscible polymer blends by *in situ* microfibrillar formation during the melt blending extrution process. On this basis, graphene/PA6 composite fibers were also prepared to investigate briefly the usage of PA6 nanofiber. The average diameter of obtained nanofibers could be smaller than 100nm. PA6 nanofibers with small size and narrow distribution could be obtained under the condition that blend ratio was 10/90-40/60 and shear rate was between 10 and 80 s^{-1}. The viscoelasticity of blends showed the dispersed phase could be fibrous. The PA6 dispersed pellets in extrusion process successively experienced molten softening, deformed into sheets or ribbons, then ribbons broken into microfibers, and at last microfibers refined to nanofibers. In the future, we will prepare PA6 nanofibers with controllable diameters based on this research and study its application in the areas of sensor, electronic equipment, filtration, absorption.

ACKNOWLEDGMENTS

This research was financially supported by the National Natural Science Foundation of China (No.20874010), the program of Introducing Talents of Discipline to Universities (No.111-2-04, B07024).

REFERENCES

1. Reneker, D. H.; Chun, I. *Nanotechnology* **1996**, *7*, 216.
2. Stoyko, F. *Compos. Sci. Technol.* **2013**, *89*, 211.
3. Nasouri, K.; Shoushtari, A. M.; Kaflou, A.; Bahrambeygi, H.; Rabbi, A. *Polym. Compos.* **2012**, *33*, 1951.
4. Zhang, J. F.; Yang, D.; Nie, J. *Polym. Adv. Technol.* **2008**, *19*, 1150.
5. Liu, P.; Zhu, K.; Xiao, R. *J. Appl. Polym. Sci.* **2013**, *130*, 2832.
6. Liu, P.; Ouyang, Y.; Xiao, R. *J. Appl. Polym. Sci.* **2012**, *123*, 2859.
7. Chao, H. X.; Dong, W.; Bei, X. *Mater. Chem. Phys.* **2010**, *124*, 48.
8. Feng, Z.; Dawud, H. *ACS Macro. Lett.* **2013**, *2*, 301.
9. Li, M.; Xiao, R.; Sun, G. *Polym. Eng. Sci.* **2011**, *51*, 835.
10. Li, Z. M.; Yang, M. B. *Mater. Res. Bull.* **2002**, *37*, 2185.
11. Li, H.; Sundararaj, U. *Macromol. Chem. Phys.* **2009**, *210*, 852.
12. Xu, H. S.; Li, Z. M. *Macromol. Mater. Eng.* **2004**, *289*, 1087.
13. Favis, B. D. *J. Appl. Polym. Sci.* **1990**, *39*, 285.
14. Scott, C. E.; Macosko, C. W. *Polymer* **1995**, *36*, 461.
15. Scott, C. E.; Macosko, C. W. *Polym. Bull.* **1991**, *26*, 341.
16. Sundararaj, U.; Macosko, C. W.; Rolando, R. *Polym. Eng. Sci.* **1992**, *32*, 1814.
17. Elemans, P. H. M.; Bos, H. L.; Janssen, J. M. H. *Chem. Eng. Sci.* **1993**, *48*, 267.
18. Rein, D. M.; Ronen, A.; Shuster, K. *Polym. Eng. Sci.* **2009**, *49*, 774.
19. Zhang, G. *J. Appl. Polym. Sci.* **2002**, *86*, 58.
20. zhang, L. Y.; Chen, G. H. *Mater. Rev.* **2011**, *25*, 85.
21. Xu, Z.; Gao, C. *Macromolecules* **2010**, *43*, 6716.
22. Du, N.; Zhao, C. Y.; Chen, Q. *Mater. Chem. Phys.* **2010**, *120*, 167.
23. Kalman, B. *Migler. Phys. Rev. Lett.* **2001**, *86*, 1023.
24. Sadhan, C.; Madhusudan, S. *Polymer* **2004**, *45*, 1665.
25. Jairo, E.; Perilla, C. *Am. Inst. Chem. Eng.* **2005**, *51*, 2675.
26. Ryan, M.; Debes, B.; Stoyko, F. *Macromol. Mater. Eng.* **2012**, *297*, 711.
27. Li, X. D. *Acta Mater. Compos. Sinica.* **1998** *2*, 62.
28. Plate, N. A.; Kulichikhin, V. G.; Talroze, R. V. *Pure Appl. Chem.* **1991**, *63*, 925.